Optics Communications 410 (2018) 559–564

Contents lists available at ScienceDirect

Optics Communications

journal homepage: www.elsevier.com/locate/optcom

Design of polarization-insensitive 2 × 2 multimode interference coupler based on double strip silicon nitride waveguides

Huimin Yang, Pengfei Zheng, Panpan Liu, Guohua Hu, Binfeng Yun *, Yiping Cui *

Advanced Photonics Center, Southeast University, Nanjing, 210096, China

ARTICLE INFO

Keywords:
Polarization-insensitive
Multimode interference coupler
Double strip silicon nitride waveguides

ABSTRACT

A polarization-insensitive 2 × 2 multimode interference coupler based on double strip silicon nitride waveguides is proposed and optimized by using the three-dimensional finite difference time domain method. By optimizing the device's structure parameters in detail, polarization independent excess loss of −0.32dB is obtained, and negligible output uniformities of −0.02dB and −0.03dB could be achieved for the TE and TM mode, respectively. The optimized polarization-insensitive 2 × 2 multimode interference coupler could be served as a building block on the double strip silicon nitride waveguides platform.

1. Introduction

Recently, the optical waveguide platform based on silicon nitride (Si_3N_4) has emerged as an alternative to the silicon on insulator (SOI) platform for integrated photonic circuits. Silicon nitride has been chosen as the dielectric waveguide material due to its low propagation loss, wide transparent window (transparent for wavelength from 0.4 μm up to 2.35 μm) and CMOS compatible fabrication [1], all of which provide the maximum flexibility from an integration standpoint [2]. Due to the above advantages, Si_3N_4 has been used to fabricate many devices [3], such as add–drop filters [4], vertical directional coupler [5], switch [6] and so on. Typically, there are three types of Si_3N_4 waveguides, including the box shape, double strip and single strip waveguides, which can be fabricated with the general CMOS fabrication process [7]. Among them, the double strip Si_3N_4 waveguide is most attractive because it can well balance the integration density and insertion loss. As far as we know, polarizing beam splitter [8], optical delay lines [9], ring resonator [10], etc. have been designed and fabricated with the double strip Si_3N_4 waveguide, while the Multimode interference (MMI) coupler based on the double strip Si_3N_4 waveguide has not been reported. And in integrated photonic platform, the MMI coupler is a basic passive building block, which can be used to construct splitter [11], Mach–Zehnder interferometer (MZI) [12], waveguide crossing [13], etc. More than this, an active MMI structure was also introduced into the active region of the super luminescent diodes (SLEDs) to reduce the thermal resistance and increase the output power, and a maximum output power of 115mW was obtained experimentally, which corresponds to a 54% improvement compared to the regular single mode SLED [14–16]. And comparing with directional couplers, MMI coupler has larger fabrication tolerance, lower optical loss, and lower polarization sensitivity [17]. Typically, the common requirements for MMI coupler are low excess loss, large optical bandwidth, small output imbalance and compact size. Until now, MMI couplers on the SOI platform have been extensively studied [18,19]. But as far as we know, the 2×2 MMI coupler based on the double strip Si_3N_4 waveguide has not been proposed and its polarization dependence has not been optimized. In this paper, a polarization-insensitive 2 × 2 MMI coupler based on the double strip Si_3N_4 waveguide was proposed and optimized by using the three-dimensional finite difference time domain method.

2. 2 × 2 MMI coupler based on double strip silicon nitride waveguide

The cross-section of the double strip Si_3N_4 waveguide used to construct 2×2 MMI is shown in Fig. 1(a), where Si_3N_4 ($n_1 = 2$) and SiO_2 ($n_2 = 1.446$) are chosen as the waveguide core and cladding materials, respectively. The height and width of the two Si_3N_4 waveguide cores are $H = 0.17$ μm and $W = 1.2$ μm, respectively. And $G = 0.5$ μm is the gap size between the two Si_3N_4 waveguide cores. The single mode condition of $W < 1.5$ μm can be obtained from the dispersion relation of the double strip Si_3N_4 waveguide at 1.55 μm wavelength as shown in Fig. 1(b). And the corresponding electric field distributions of the fundamental TE and TM modes are shown in Fig. 1(c) and Fig. 1(d), respectively.

* Corresponding authors.
E-mail addresses: ybf@seu.edu.cn (B. Yun), cyp@seu.edu.cn (Y. Cui).

https://doi.org/10.1016/j.optcom.2017.11.003
Received 30 August 2017; Received in revised form 28 October 2017; Accepted 2 November 2017
Available online 20 November 2017

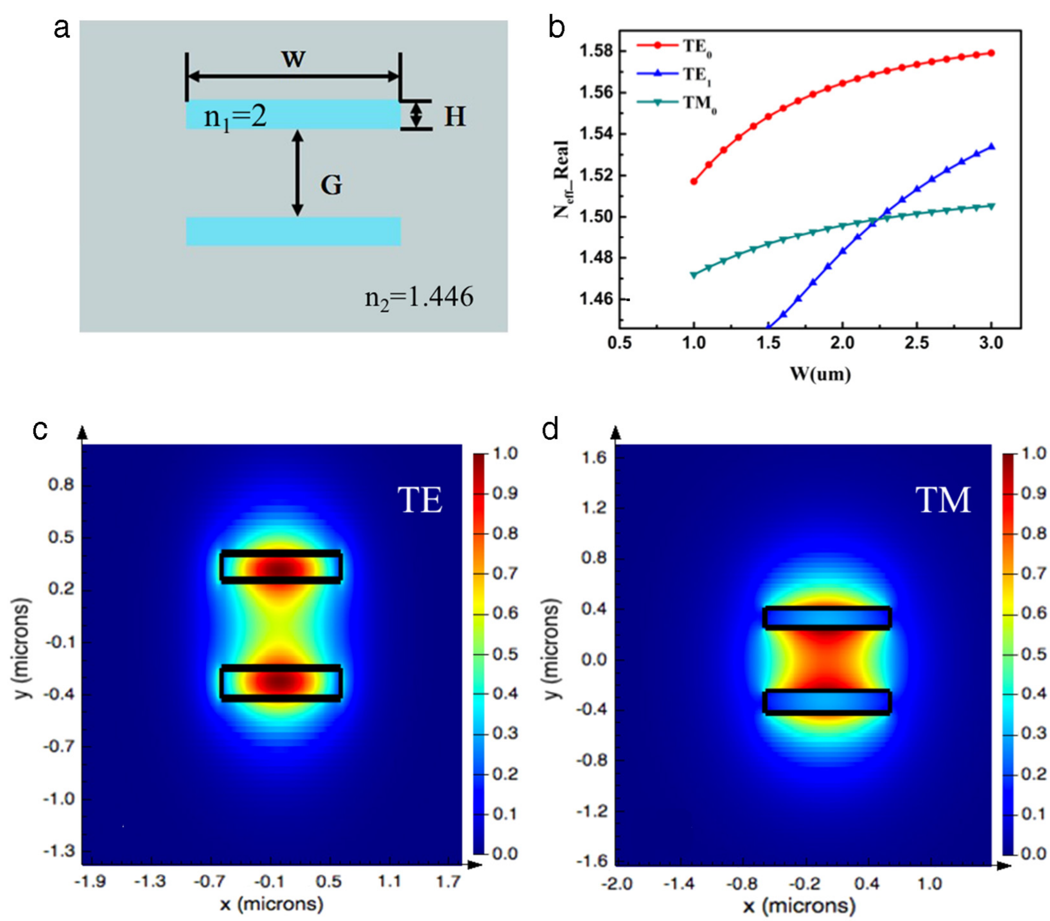

Fig. 1. (a) The waveguide cross-section of the double strip Si_3N_4waveguide. (b) The mode dispersion relation of the double strip Si_3N_4 waveguide. (c) $|E|^2$ distribution of the fundamental TE mode. (d) $|E|^2$ distribution of the fundamental TM mode.

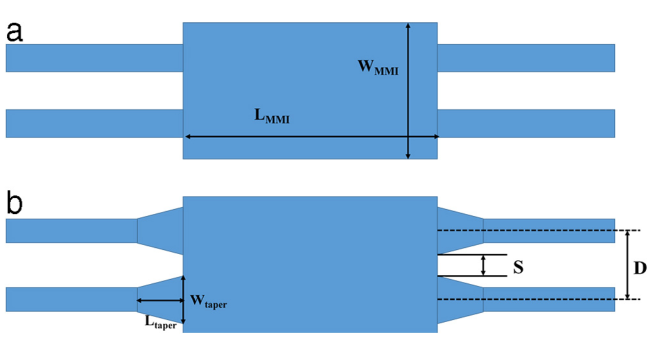

Fig. 2. (a) Conventional 2 × 2 MMI. (b) Optimized 2 × 2 MMI with linear tapers.

It is well known the working mechanism of MMI coupler is the self-imaging effect, where an input optical field profile is reproduced in single or multiple images at periodic intervals along the propagation direction [20]. A typical structure of 2 × 2 MMI coupler is shown in Fig. 2(a), where W_{MMI} and L_{MMI} are the width and length of the MMI region, respectively. A serious mode mismatch loss will occur at the junction between the single mode input/output waveguides and the MMI region. In order to reduce this mode mismatch loss, four linear taper waveguides were added between the input/output waveguides and the MMI region, just as shown in Fig. 2(b), where W_{taper} and L_{taper} are the width and length of the taper.

A fundamental mode in one of the input ports can stimulate a set of modes ϕ_m in the MMI region ($m = 0, \ldots, M-1$), with the mode propagation constants $\beta_m = 2\pi n_{\mathrm{eff,m}}/\lambda$, where $n_{\mathrm{eff,m}}$ is the effective mode index of the m order mode. For perfect (error-free) imaging, it is required that mode propagation constants satisfied the following relationship [20,21]:

$$\Delta\beta_m = \beta_0 - \beta_m = \frac{m(m+2)\pi}{3L_\pi} \tag{1}$$

Where $L_\pi = \pi/(\beta_0\text{-}\beta_1)$ is the beat length between the two lowest order modes, which can be rewritten as:

$$L_\pi(\lambda) = \frac{\lambda}{2\left[n_{eff,0}(\lambda) - n_{eff,1}(\lambda)\right]} \tag{2}$$

Which can be approximated as:

$$L_\pi(\lambda) \approx \frac{4n_{eff,0}W_{\mathrm{MMI}}^2}{3\lambda} \tag{3}$$

Where $n_{\mathrm{eff,0}}$ is the fundamental mode effective index of MMI region.

The three interference types in the MMI region are the general interference, paired interference and symmetric interference, respectively. In order to make the device compact, the proposed 2 × 2 MMI coupler is based on the paired interference, which can reduce the length of the MMI coupler to $L_{\mathrm{MMI}} = L\pi/2$, which is 1/3 of the general interference length [21]. And according to the self-image principle [20], the input and output waveguides of the 2×2 MMI coupler with 3dB splitting ratio should be located at $W_e/3$ and $2W_e/3$ of the MMI region, respectively. Where W_e is the effective width of the MMI region and is approximately equal to the width of MMI region:

$$W_{\mathrm{MMI}} \approx W_e = 3D \tag{4}$$

$$D = S + W_{taper} \tag{5}$$

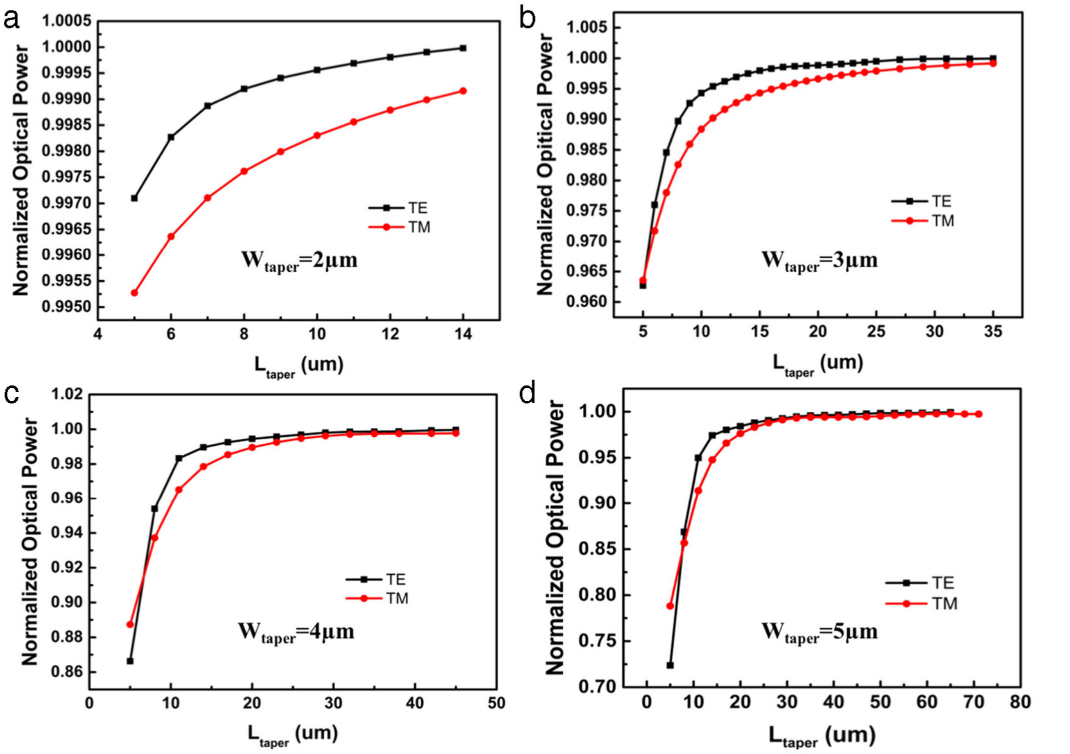

Fig. 3. The relation between the mode mismatch loss and the linear taper length. (a) $W_{\text{taper}} = 2$ μm. (b) $W_{\text{taper}} = 3$ μm. (c) $W_{\text{taper}} = 4$ μm. (d) $W_{\text{taper}} = 5$ μm.

Where D is the center to center distance between two input/output waveguides. And in order to lower the fabrication costs, a minimum gap size of $S = 2$ μm is chosen, which can be achieved with conventional contact lithography. A set of W_{MMI} (12 μm, 15 μm, 18 μm, 21 μm) were chosen to optimize the polarization dependences of the proposed MMI coupler, and according to Eqs. (4) and (5), the corresponding W_{taper} of 2 μm, 3 μm, 4 μm and 5 μm were obtained, respectively. And adiabatic taper is added to avoid the mode mismatch loss between the single mode input/output waveguide and the MMI region. The adiabatic tapers for the four W_{taper} cases were optimized and the results are shown in Fig. 3. And in order to keep the mode mismatch loss less than 0.01%, the optimized L_{taper} was chosen as 14 μm, 30 μm, 35 μm, 60 μm when W_{taper} is 2 μm, 3 μm, 4 μm, 5 μm, respectively.

Because n_1 and G are constant as shown in Fig. 1(a), therefore the polarization characteristics of the proposed 2 × 2 MMI based on the double strip Si_3N_4 waveguide only depend on W_{MMI}. It is well known that the difference between the beat lengths L_π of the two polarizations should be zero ($\Delta L_\pi = L\pi(TE)\text{-}L_{\pi(\text{TM})} = 0$) for a polarization insensitive MMI coupler [22]. So the relationship between W_{MMI} and L_π of the two polarizations was simulated and the results are shown in Fig. 4.

From Ref. [22], it is well known that the requirement of obtaining a polarization independent MMI is the beat lengths (L_π) of the two polarizations are equal ($\Delta L_\pi = L_\pi(TE) - L_\pi(\text{TM}) = 0$). In other words, the two-fold imaging positions $L_{\text{MMI}}= L_\pi/2$ of the two polarizations should be equal, too. But with the inherent polarization dependence of the multimode waveguide caused by the different waveguide width and waveguide height, the two-fold imaging positions of the TE and TM modes are different, which can be shown in Fig. 4. This is the main reason why the proposed 2 × 2 MMI based on the double strip Si_3N_4 waveguides cannot be completely polarization-independent, which needs L_{MMI} of the two polarizations be equal. The polarization dependence of the adiabatic taper waveguide is also a reason that makes the proposed MMI not completely polarization-independent. From Fig. 3, it can be observed that if we further increase the taper length, the taper polarization dependence of TE and TM mode will decrease thus the polarization dependence of the proposed MMI will be even decreased. But the increased taper length will increase the device size, which is not beneficial for high density integration. In order to decrease the polarization dependence of the proposed MMI coupler, the excess loss and the output uniformity were chosen to characterize the device's polarization dependence.

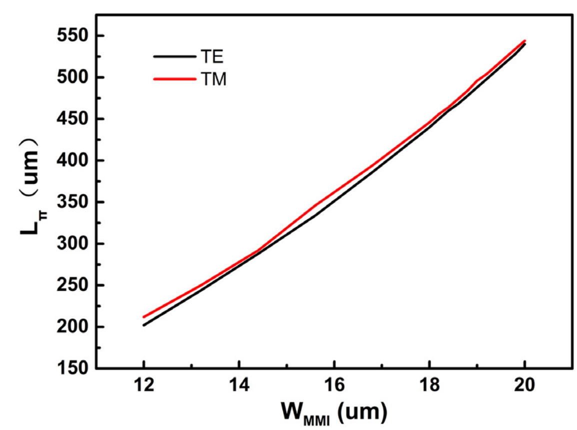

Fig. 4. The relationship between W_{MMI} and L_π of the two polarizations.

$$Excess\ Loss = 10Log\left(\frac{P_{out}}{P_{in}}\right) \tag{6}$$

$$Uniformity = 10Log\left(\frac{P_{\min}}{P_{\max}}\right) \tag{7}$$

Where P_{out} is the total optical power of the two output ports, P_{min} and P_{max} are the minimum and maximum output power of two output ports, respectively. The excess loss and the output uniformity of the 2×2 MMI coupler with different L_{MMI} were simulated and shown in Fig. 5.

In Figs. 5(a, c, e, g), it is obvious that the minimum excess losses of both the fundamental TE and TM modes decrease when W_{MMI} increases.

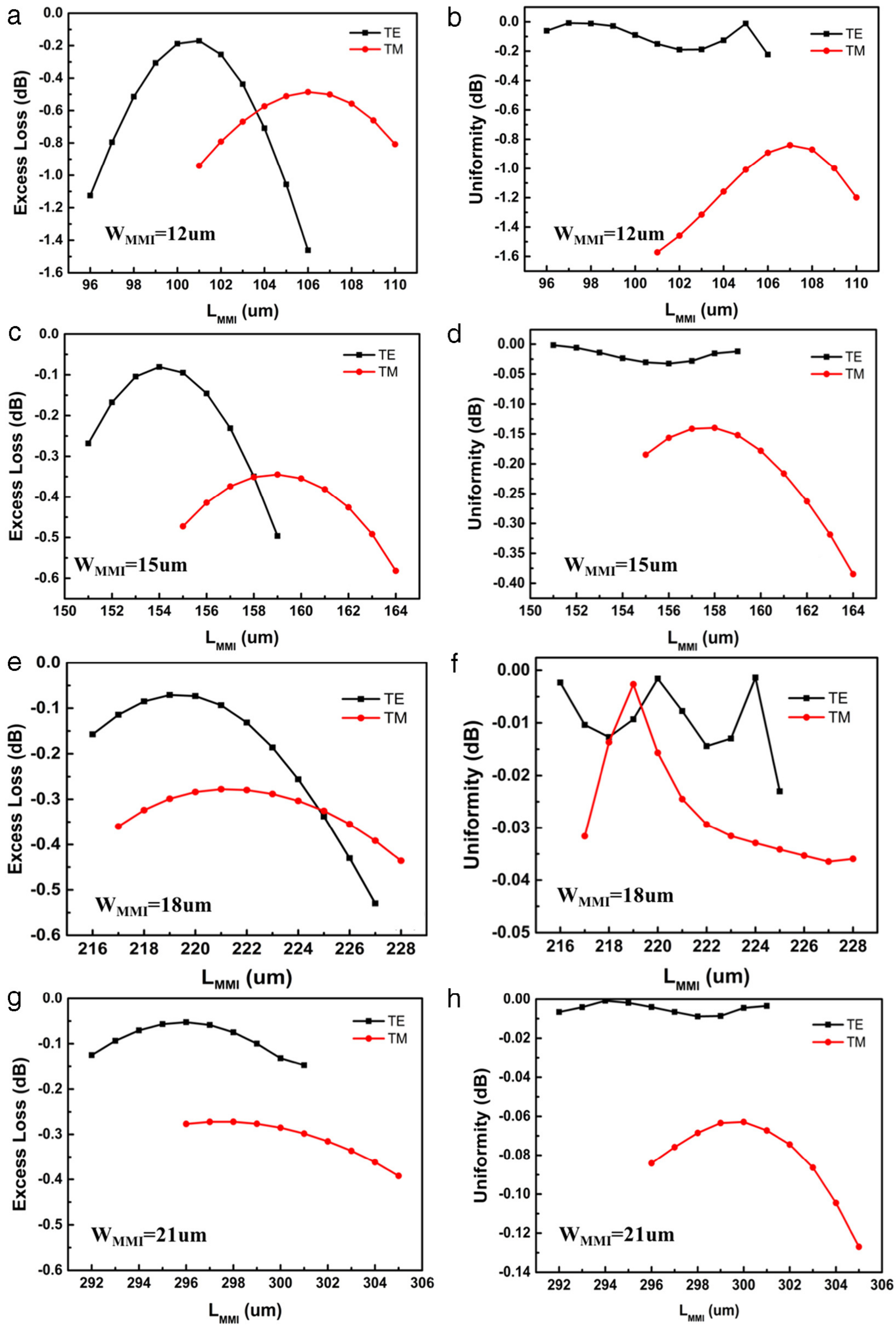

Fig. 5. (a, c, e, g) The relation between the excess loss and L_{MMI} with different W_{MMI}. (b, d, f, h) The relation between the uniformity and L_{MMI} with different W_{MMI}.

And when W_{MMI} was chosen as 12 μm, 15 μm, 18 μm, equal excess losses of the fundamental TE and TM mode can be obtained when L_{MMI} is 103.6 μm, 158 μm and 224.8 μm, respectively. So at these conditions the 2 × 2 MMI coupler can be considered as excess loss polarization insensitive. But when W_{MMI} = 21 μm, it is difficult to achieve excess loss polarization insensitive as shown in Fig. 5(g). On the other hand, the output uniformity is also a polarization dependent parameter of the MMI coupler, which needs to be optimized. As shown in Figs. 5(b, d, f, h), the output uniformities of both the TE and TM modes decrease when W_{MMI} increases. And for the case of L_{MMI} = 224.8 μm and W_{MMI} = 18 μm, which corresponds to the excess loss polarization insensitive condition shown in Fig. 5(e), the obtained output uniformity is as low as −0.02 dB and −0.03 dB for the TE and TM mode, respectively. According to the self-imaging principle of the MMI,

Table 1
The optimized device parameters.

W_{MMI}	L_{MMI}	S	D	W_{taper}	L_{taper}
18 μm	224.8 μm	2 μm	6 μm	4 μm	35 μm

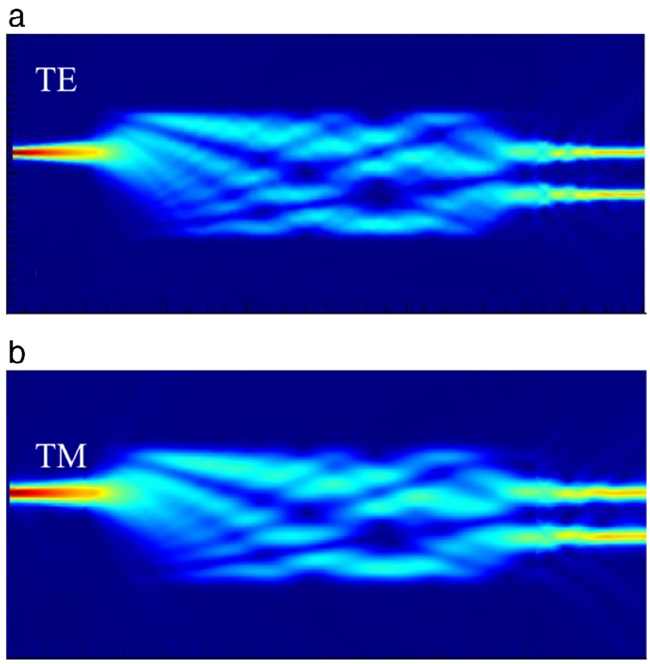

Fig. 6. The | E|^2 distribution of the optimized MMI coupler for the (a) TE mode (b) TM mode.

the larger W_{MMI} is, the more waveguide modes could be excited in the multimode region. And by exciting more waveguide modes, the two-fold imaging could be much more similar with the incident optical mode field because the self-imaging could be regarded as a sum of the weighted modes in the multimode waveguide [20]. With this improved two-fold imaging quality, the excess loss could even be reduced. But in the other hand, the polarization-dependence will increase because the multimode waveguide becomes much more asymmetric. So here W_{MMI} = 18 μm was chosen to balance this tradeoff. Based on the above results, an approximate polarization-independent 2 × 2 MMI based on double strip Si_3N_4 waveguides can be obtained with the optimized device parameters shown in Table 1.

With the optimized structure parameters shown in Table 1, the TE and TM electric field distributions in the optimized MMI coupler are shown in Fig. 6. With the adiabatic taper, both the fundamental TE and TM modes can effectively excite multiple modes in the multimode waveguide with negligible mode mismatch loss. And according to the self-imaging principle, a two-fold imaging is formed at the end of the multimode waveguide, where negligible radiation loss is obtained by using two output waveguides with adiabatic tapers. Besides, with the polarization independent optimization, good output uniformities are obtained for the TE and TM mode simultaneously. With the optimized structure parameters, a polarization-independent excess loss of −0.32 dB is obtained, and negligible output uniformities of −0.02 dB and −0.03 dB could be achieved for the TE and TM mode, respectively. It shows the good performance of the proposed MMI.

Finally, the wavelength dependence of the proposed MMI is also investigated the results are shown in Fig. 7. In the wavelength range of 1.52 μm~1.57 μm, the excess loss is −0.098 dB~−0.538 dB and −0.247 dB~−0.416 dB for the TE and TM mode, respectively.

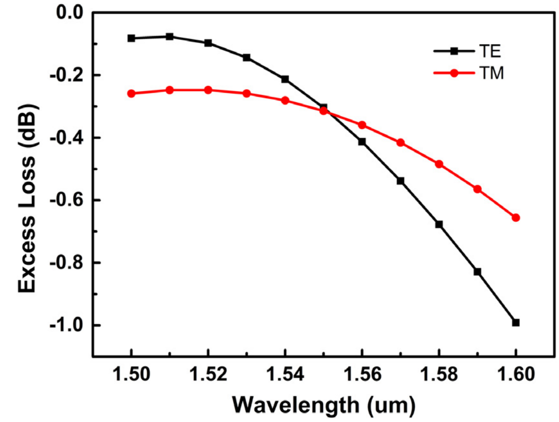

Fig. 7. Excess loss for TE and TM modes versus wavelength.

3. Conclusion

In summary, polarization-insensitive 2 × 2 MMI coupler based on the double strip Si_3N_4 waveguides was proposed. According to silicon nitride double strip waveguides structure characteristics, we studied and optimized the polarization dependence of the 2 × 2 MMI coupler based on double strip silicon nitride waveguides. Finally, an optimized polarization-insensitive 2 × 2 MMI coupler was obtained when W_{MMI} = 18 μm and L_{MMI} = 224.8 μm are satisfied, the achieved polarization-insensitive excess loss is −0.32 dB, and the output uniformity was −0.02 dB and −0.03 dB for the TE and TM mode, respectively.

Acknowledgment

This work was supported by the National Science Foundation of Jiangsu Province under Grant [number BK 20161429].

References

[1] Q. Zhao, S. Campione, F. Capolino, O. Boyraz, Experimental demonstration of directive Si_3N_4 optical leaky wave antenna with semiconductor perturbations, Proc. SPIE Int. Soc. Opt. Eng. PP (99) (2015) 1–1.
[2] R. Heideman, M. Hoekman, E. Schreuder, Triplex-based integrated optical ring resonators for lab-on-a-chip and environmental detection, IEEE J. Sel. Top. Quant. 18 (5) (2012) 1583–1596.
[3] Y. Wang, J. Wang, C. Sun, B. Xiong, A simple fabrication process for SiNx/SiO2 waveguide based on sidewall oxidation of patterned silicon substrate, IEEE Opto-Electron. Commun. Conf. 38 (2015) 1–3.
[4] T. Barwicz, M.A. Popović, M.R. Watts, P.T. Rakich, E.P. Ippen, H.I. Smith, Fabrication of add-drop filters based on frequency-matched microring resonators, J. Lightwave Technol. 24 (5) (2006) 2207–2218.
[5] D.D. John, M.J.R Heck, J.F. Bauters, R. Moreira, Multilayer platform for ultra-low-loss waveguide applications, IEEE Photonic Technol. Lett. 24 (11) (2012) 876–878.
[6] L.A. Shiramin, D.V. Thourhout, Graphene modulators and switches integrated on silicon and silicon nitride waveguide, IEEE J. Sel. Top. Quant. (2016) 1–1.
[7] C.G.H. Roeloffzen, L. Zhuang, C. Taddei, A. Leinse, R.G. Heideman, P.W.L. van Dijk, R.M. Oldenbeuving, D.A.I. Marpaung, M. Burla, K.J. Boller, Silicon nitride microwave photonic circuits, Opt. Express 21 (2013) 22937–22961.
[8] Jijun Feng, Ryoichi Akimoto, A three-dimensional silicon nitride polarizing beam splitter, IEEE Photonic Technol. Lett. 26 (7) (2014) 706–709.
[9] Leimeng Zhuang, David Marpaung, Maurizio Burla, Willem Beeker, Arne Leinse, Chris Roeloffzen, Low-loss, high-index-contrast Si_3N_4/SiO_2 optical waveguides for optical delay lines in microwave photonics signal processing, Opt. Express 23 (19) (2011) 23162.
[10] Leimeng Zhuang, Willem Beeker, Arne Leinse, René Heideman, Novel wideband microwave polarization network using a fully-reconfigurable photonic waveguide interleaver with a two-ring resonator- assisted asymmetric Mach–Zehnder structure, Opt. Express 21 (3) (2013) 3114.
[11] Q. Wang, S. He, L. Wang, A low-loss Y-branch with a multimode waveguide transition section, IEEE Photonic Technol. Lett. 14 (2002) 1124–1126.
[12] D.J. Thomson, G.T.R.Y. Hu, J. Fedeli, Low loss MMI couplers for high performance MZI modulators, IEEE Photonic Technol. Lett. 22 (2010) 1485–1487.

[13] S. Kim, G. Cong, H. Kawashima, T. Hasama, H. Ishikawa, Tilted MMI crossings based on silicon wire waveguide, Opt. Express 22 (2014) 2545–2552.
[14] Zhigang Zang, Keisuke Mukai, Paolo Navaretti, Marcus Duelk, Christian Velez, Kiichi Hamamoto, Thermal resistance reduction in high power superluminescent diodes by using active multi-mode interferometer, Appl. Phys. Lett. 100 (2012) 031108.
[15] Zhigang Zang, Takahiro Minato, Paolo Navaretti, Yasuhiro Hinokuma, Marcus Duelk, Christian Velez, Kiichi Hamamoto, High-power (>110 mW) superluminescent diodes by using active multimode interferometer, IEEE Photonic Technol. Lett. 22 (2010) 721–723.
[16] Zhigang Zang, Keisuke Mukai, Paolo Navaretti, Marcus Duelk, Christian Velez, Kiichi Hamamoto, High power and stable high coupling efficiency (66%) superluminescent light emitting diodes by using active multi-mode interferometer, IEICE Trans. Electron. (2011) 862–864.
[17] Y. Shao, X. Han, X. Han, Z. Lu, Z. Wu, J. Teng, et al., Optimal design of 850 nm 2×2 multimode interference polymer waveguide coupler by imprint technique, Photonic Sensors 6 (3) (2016) 234–242.
[18] D.X. Xu, S. Janz, P. Cheben, Design of polarization-insensitive ring resonators in silicon-on-insulator using MMI couplers and cladding stress engineering, IEEE Photonic Technol. Lett. 18 (2) (2016) 343–345.
[19] D. Dai, S. He, Optimization of ultra-compact polarization-insensitive multimode interference couplers based on Si nanowire waveguides, IEEE Photonic Technol. Lett. 18 (19) (2010) 2017–2019.
[20] L.B. Soldano, E.C.M. Pennings, Optical multi-mode interference devices based on self-imaging: Principles and applications, J. Lightwave Technol. 13 (4) (1995) 615–627.
[21] A. Maesenovo, A. Ortegamoñux, D. Pérezgalacho, I. Molinafernández, J.G. Wangüem ertpérez, L. Zavargopeche, et al., Wavelength independent multimode interference coupler, Opt. Express 21 (6) (2013) 7033.
[22] Daoxin Dai, Sailing He, Daoxin Dai Sailing He Optimization of ultracompact polarization- insensitive multimode interference couplers based on Si nanowire waveguides, IEEE Photonic Technol. Lett. 18 (19) (2006) 2017–2019.